IMPLEMENTATION OF SPECTRAL MODELS FOR GAS RADIATION INTO THE CFD SOLVER NSMB AND VALIDATION ON THE BASIS OF THE SSME MAIN COMBUSTION CHAMBER

F. Göbel, Institute of Thermodynamics, Universität der Bundeswehr München,
D-85577 Neubiberg/Munich, Germany

Abstract

This work is intended to identify models that approximate the spectral properties of combustion gases for thermal gas radiation and implement them in the CFD code NSMB. The Weighted Sum of Gray Gases Model (WSGGM) formulated by Smith, Copalle and Johansson as well as the Spectral Line Weighted Sum of Gray Gases Models (SLWSGGM) formulated by Denison are investigated. The theoretical basis of all models is presented, followed by a quantitative comparison in terms of total emissivity predicted by these models. Finally a CFD simulation of the Space Shuttle Main Engine (SSME) Main Combustion Chamber (MCC) is realised with different WSGG models and the SLWSGGM for H_2/O_2 and CH_4/O_2 combustion using the CFD codes NSMB and CFX. The investigation of total emissivity reveals a strong limitation of all models in temperature. The CFD simulation confirms the assumption that those models predicting a higher total emissivity also compute a higher radiative heat flux. For the H_2/O_2 case the models of Smith and Denison provide the best results compared to benchmark data whereas for CH_4/O_2 Copalle's and Denison's models are most suitable. Concerning computational effort, the models by Smith, Copalle and Johansson are identified to be the least time consuming models.

NOMENCLATURE

Latin Symbols:

a	$[1/\mathrm{m}]$	Absorption coefficient
A	$[-]$	Polynomial coefficient
b	$[-]$	Polynomial coefficient
B	$[-]$	Polynomial coefficient
C_{abs}	$[\mathrm{m}^2/\mathrm{mol}]$	Absorption cross section
F	$[-]$	Absorption line blackbody distribution function
f	$[-]$	Arbitrary function
G	$[\mathrm{W}/\mathrm{m}^2]$	Incident radiation
i	$[\mathrm{W}/\mathrm{m}^2\,\mathrm{sr}]$	Radiation intensity
I	$[-]$	Number of gray gases
j	$[-]$	Counting index
J	$[-]$	Number of intervals for one gray gas / Order of polynomial
K	$[-]$	Number of species
l	$[-]$	Summation index
m	$[-]$	Summation index
n	$[-]$	Summation index
p	$[\mathrm{Pa}]$	Static pressure
P_F	$[-]$	Correlation function
q	$[\mathrm{W}/\mathrm{m}^2]$	Heat flux
R_m	$[\mathrm{J}/\mathrm{kg\,mol}]$	Gas constant
s	$[\mathrm{m}]$	Direction
S	$[\mathrm{m}]$	Path length
T	$[\mathrm{K}]$	Static temperature
w	$[-]$	Weight of gray gas
X	$[-]$	Molar fraction

Greek Symbols:

ε	$[-]$	Total emissivity
λ	$[\mathrm{m}]$	Wavelength
ξ	$[-]$	Logarithm of absorption cross section
σ	$[1/\mathrm{m}]$/ $[\mathrm{W}/\mathrm{m}^2\,\mathrm{K}^4]$	Scattering coefficient / Stefan- Boltzmann constant
ϕ	$[-]$	Scattering phase function
ψ	$[-]$	Logarithm of elevated pressure
ω	$[\mathrm{sr}]$	Solid angle

Subscripts:

abs	Absorption
b	Blackbody property / Broadening
g	Gas
i	Index of direction / Index of gray gas
k	Index of species
p	Pressure based
rad	Radiation
ref	Reference state
sb	Self broadening
λ	Spectral value
0	Clear gas property

Superscripts:

j	Index for gray gas interval
lower	Lower boundary of gray gas interval

upper	Upper boundary of gray gas interval

Abbreviations and Acronyms:

CFD	Computational Fluid Dynamics
DTM	Discrete Transfer Model
FSK	Full Spectrum k-Distribution
MCC	Main Combustion Chamber
RRM	Rosseland Radiation Model
RTE	Radiative Transfer Equation
RWHF	Radiative Wall Heat Flux
SLWSGGM	Spectral Line Weighted Sum of Gray Gases Model
SSME	Space Shuttle Main Engine
WSGGM	Weighted Sum of Gray Gases Model

1. INTRODUCTION

Within a simulation of radiative heat transfer, several difficulties have to be overcome. One of them is the modelling of radiative properties of the participating media. These radiative properties depend on wavelength, adding a further dimension to the Radiative Transfer Equation (RTE) [1], p.3.

With an approximate solution of the RTE, a spectral integration to gain total values can be replaced by a summation if regions in the wavelength spectrum are known in which the properties are constant, hence do not depend on the wavelength (gray gas). This is the basic idea behind the Weighted Sum of Gray Gases Model (WSGGM), originally introduced by Hottel [2]. The radiative property consists of a weighted sum of gray gas properties, which are independent of wavelengths [2], p.247. It has been shown that the WSGGM can be used with any approximation technique of the RTE [1], p. 615.

The Space Shuttle Main Engine (SSME) Main Combustion Chamber (MCC) is a well analysed rocket motor whose radiative heat transfer has been investigated numerically by several research groups in the past [3,4]. They discover that the radiative wall heat flux in the SSME MCC can be 10 % of the total wall heat flux with the typical H_2/O_2 combustion. Recently, these results have been reproduced by [5] using the WSGGM by Smith [6]. They also investigate the combustion in the SSME MCC using CH_4/O_2 as propellant and the WSGGM by Copalle [8], concluding that the radiative wall heat flux increases compared to H_2/O_2 [7].

Using other WSGG models or the more sophisticated SLWSGGM by Denison and Webb [9], the accuracy of the CFD simulations is expected to increase. The SLWSGGM is assessed by Modest [1], p.615 to be one of the most appropriate WSGG models since it bases on the spectral data of a gas instead of a regression scheme [1], p. 615.

2. THEORETICAL CONSIDERATIONS

2.1. Theory of Radiative Transfer

The basis of all radiative considerations is the Radiative Transfer Equation (RTE) in its spectral form [10], p.562

$$\frac{di_\lambda}{ds} = \underbrace{a_\lambda \cdot i_{\lambda b}(s)}_{A} - \underbrace{\left(a_\lambda + \sigma_\lambda\right) \cdot i_\lambda(s)}_{B} + \underbrace{\frac{\sigma_\lambda}{4\pi} \cdot \int_{4\pi} i_\lambda(s,\omega_i) \cdot \phi_\lambda(\omega_i,\omega) d\omega_i}_{C} \quad (1)$$

The RTE in Eq. (1) describes the change in intensity of a beam passing through a medium in the direction s. The change is due to a gain of intensity by emission and scattering (A & C) and a loss of intensity by absorption and scattering (B).

The RTE is an integro-differential equation depending on 3 spatial, 2 directional and 1 spectral variables, which makes an analytical solution almost impossible for most engineering applications. Thus, the RTE has to be solved numerically using radiation transport models.

With the spectral intensity i_λ given as the solution of the RTE, the divergence of the spectral radiative heat flux can be calculated [10], p.570

$$\nabla q_{\mathrm{rad},\lambda} = a_\lambda \cdot \left(4 \cdot \pi \cdot i_{\lambda b} - G_\lambda\right). \quad (2)$$

In Eq. (2), the spectral incident radiation G_λ is given by

$$G_\lambda = \int_{4\pi} i_\lambda \, d\omega. \quad (3)$$

The divergence of the total radiative heat flux, necessary to couple the radiative heat transfer with the energy equation in CFD simulations, is obtained by integration of the spectral value over wavelength

$$\nabla \vec{q}_{\mathrm{rad}} = \int_0^\infty \vec{\nabla} \vec{q}_{\mathrm{rad},\lambda} \, d\lambda. \quad (4)$$

Figure 1 shows that the absorption coefficient varies strongly over wavelength and can have several different values. Therefore integration over wavelength in Eq. (4) increases computational costs. This problem can be overcome using models that approximate the spectral dependency of the absorption coefficient and hence minimize computational efforts, replacing the integration in Eq. (4) by a summation. One of these spectral models is known as

the Weighted Sum of Gray Gases Model (WSGGM).

2.2. Theory of the WSGGM approach

The simplifying approach of the WSGGM is to subdivide the entire spectrum into J regions $\Delta\lambda_i^j$ in which the absorption coefficient is assumed to have the constant value a_i. As the absorption coefficient is no longer dependent on the wavelength in this region it fulfils the requirements of a gray gas, which gives the model its name.

Additionally to the gray gases, those regions in the spectrum in which the absorption coefficient is zero are represented by a clear gas denoted by index $i = 0$

(5) $a_0 = 0$.

Figure 1 shows the regions for one gray gas and $J = 3$.

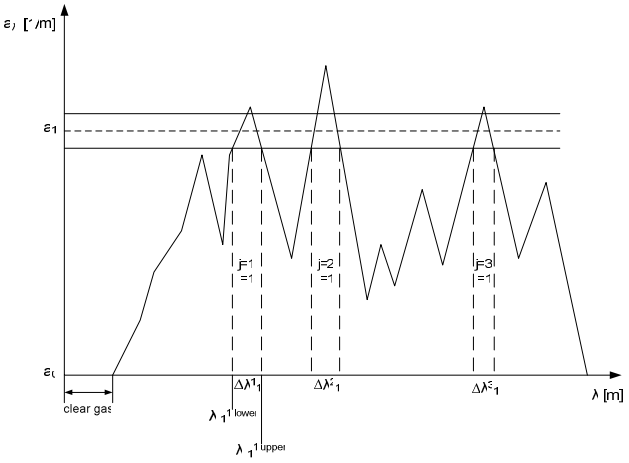

FIGURE 1. Absorption coefficients a_λ & a_1, wavelengths $\lambda_i^{j,\text{lower}}$ & $\lambda_i^{j,\text{upper}}$ and wavelengths intervals $\Delta\lambda_i^j$ for one gray gas (*I*=1) and three regions in the spectrum (*J*=3)

To estimate the share of the gray gas' absorption coefficient in the total spectrum, a blackbody weight is introduced. This weight indicates the ratio of blackbody intensity in the regions $\Delta\lambda_i^j$ divided by the blackbody intensity in the entire spectrum

(6) $$w_i = \frac{i_{i,\mathrm{b}}}{\int_0^\infty i_{\lambda\mathrm{b}} d\lambda} = \frac{\sum_{j=1}^{J} \int_{\lambda_i^{j,\text{lower}}}^{\lambda_i^{j,\text{upper}}} i_{\lambda\mathrm{b}} d\lambda}{\int_0^\infty i_{\lambda\mathrm{b}} d\lambda}.$$

Figure 2 depicts this calculation for $J = 3$.

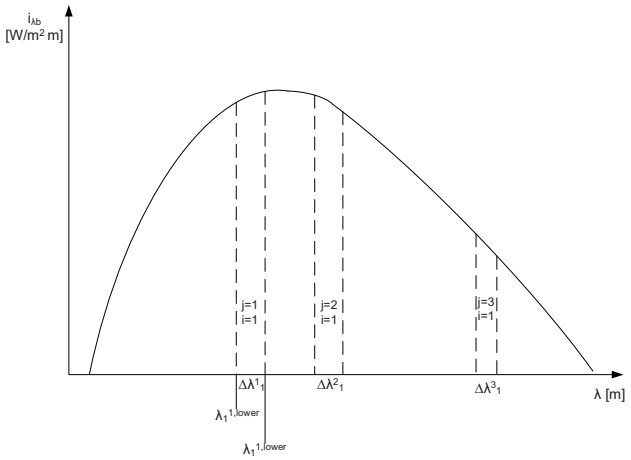

FIGURE 2. Blackbody intensity $i_{\lambda b}$, wavelengths $\lambda_i^{j,\text{lower}}$ & $\lambda_i^{j,\text{upper}}$ and wavelengths intervals $\Delta\lambda_i^j$ for one gray gas (*I*=1) and three regions in the spectrum (*J*=3)

Equation (6) can be simplified, assuming a refractive index of unity

(7) $$\int_0^\infty i_{\lambda\mathrm{b}} d\lambda = \frac{\sigma \cdot T^4}{\pi}.$$

With this, the blackbody weight becomes

(8) $$w_i = \frac{i_{i,\mathrm{b}}}{\int_0^\infty i_\lambda d\lambda} = \frac{i_{i,\mathrm{b}}}{\frac{\sigma \cdot T^4}{\pi}}.$$

The weights of all gray gases and the clear gas have to fulfil the constraint

(9) $$\sum_{i=0}^{I} w_i(T) = 1,$$

leading to a constitutive equation for the weight of the clear gas

(10) $$w_0 = 1 - \sum_{i=1}^{I} w_i(T).$$

To illustrate the role of the blackbody weight, consider an absorption coefficient with a corresponding weight $w_i = 0.25$. This means that 25% of all absorption coefficients in the entire spectrum have a value of a_i.

Using the WSGGM, the RTE of Eq. (1) yields values for the intensity i_i corresponding to each gray gas. Hence, the divergence of the total radiative heat flux

can be approximated as

$$\nabla \vec{q}_{\mathrm{rad}} \approx \sum_{i=1}^{I} \nabla \vec{q}_{\mathrm{rad},i} \,, \tag{11}$$

with the divergence of the radiative heat flux for each gray gas

$$\nabla q_{\mathrm{rad},i} = a_i \cdot \left(4 \cdot w_i \cdot \sigma \cdot T^4 - G_i\right). \tag{12}$$

The incident radiation G_i in Eq. (12) depends on the intensity as solution of the RTE

$$G_i = \int_{4\pi} i_i \, d\omega. \tag{13}$$

3. SURVEY OF WSGG MODELS

3.1. WSGGM by Smith

The WSGGM by Smith bases on a regression scheme to total emissivity data from the exponential wide band model [6], p. 604.

The absorption coefficient can be calculated by

$$a_i = a_{p,i} \cdot \sum_{k=0}^{K} X_k \cdot p \,, \tag{14}$$

whereas the pressure based absorption coefficients $a_{p,i}$ are given in [6], p. 606. The weight for the i-th gray gas is then obtained by the polynomial of J-th order

$$w_i(T) = \sum_{j=1}^{J} b_{i,j} \cdot T^{j-1} \,, \tag{15}$$

with coefficients $b_{i,j}$ also given in [6], p. 606. The model is limited to certain temperatures and pressure path lengths $p \cdot S$, as indicated in Table 1.

3.2. WSGGM by Copalle

The WSGGM by Copalle is similar to the one by Smith as it fits its data to total emissivity results from the exponential wide band model [8], p.101. Hence, the absorption coefficient can be calculated with Eq. (14) and the weight is given by a first order polynomial

$$w_i = b_{i,1} + b_{i,2} \cdot T \,. \tag{16}$$

Values of pressure based absorption coefficient $a_{p,i}$ as well as of $b_{i,1}$ and $b_{i,2}$ are given in [8], p.107. Limitations are given in Tab. 1.

3.3. WSGGM by Johansson

Johansson's WSGGM is the most recent model based on a regression scheme [11]. In contrast to former models, it considers the molar fractions of the combustion species H_2O and CO_2 and uses four gray gases instead of three. This influences the pressure based absorption coefficient for use in Eq. (14).

$$a_{p,i} = f\left(\frac{X_{H_2O}}{X_{CO_2}}\right) = A_i + B_i \cdot \frac{X_{H_2O}}{X_{CO_2}} \,, \tag{17}$$

as well as its corresponding weight

$$w_i(T) = \sum_{j=1}^{J} b_{i,j} \cdot \left(\frac{T}{T_{\mathrm{ref}}}\right)^{j-1} \,, \tag{18}$$

With $T_{\mathrm{ref}} = 1200K$ and the polynomial coefficient

$$b_{i,j} = f\left(\frac{X_{H_2O}}{X_{CO_2}}\right) = A_{i,j} + B_{i,j} \cdot \frac{X_{H_2O}}{X_{CO_2}} \,. \tag{19}$$

Coefficients A_i, B_i, $A_{i,j}$ and $B_{i,j}$ can be found in [11], the limits of temperature and pressure path length are printed in Tab. 1.

3.4. SLWSGGM by Denison/Webb

The Spectral Line Weighted Sum of Gray Gases Model (SLWSGGM) Model has been developed by Denison and Webb based on line-by-line spectral data from HITRAN 1991, [9], p.501. The absorption coefficient for the i-th gray gas is given as a function of the absorption cross section and the molar density of a species

$$a_i = \overline{C_{\mathrm{abs,i}}} \cdot \frac{X \cdot p}{R_{\mathrm{m}} \cdot T} \,, \tag{20}$$

with the mean absorption cross section defined as

$$\overline{C_{\mathrm{abs},i}} = \sqrt{C_{\mathrm{abs},i+1}(T) \cdot C_{\mathrm{abs},i}(T)} \,. \tag{21}$$

In contrast to the other WSGG models, the absorption cross section (and thus the absorption coefficient) can be chosen freely.

The weight of the gray gas can then be evaluated as

$$w_i = F_{i+1} - F_i \,, \tag{22}$$

with an absorption line blackbody distribution func-

tion, in this work correlated by [9], p.504

(23)

$$F_i(T_g,T_b,\xi_i-\xi_{sb}) = \frac{1}{2}\cdot\tanh\left[P_F\left(T_g,T_b,\xi_i-\xi_{b/sb,i}\right)\right]+\frac{1}{2}.$$

The function P_F is represented by another correlation including the temperature and the absorption cross section

(24)

$$P_F = \sum_{l=0}^{3}\sum_{m=0}^{3}\sum_{n=0}^{3} b_{lmn}\cdot\left(\frac{T_g}{2500}\right)^n\cdot\left(\frac{T_b}{2500}\right)^m\cdot\left(\xi_i-\xi_{b/sb,i}\right)^l,$$

with

(25) $$\xi_i = \ln\left(\overline{C_{abs,i}}\right),$$

and for H_2O systems with respect to self-broadening at atmospheric pressure

(26) $$\xi_{sb,i} = \sum_{l=0}^{3}\sum_{m=0}^{3}\sum_{n=0}^{2} c_{lmn}\cdot\left(\frac{T_b}{2500}\right)^n\cdot\xi_i^m\cdot X_{H_2O}^{\,l+1}.$$

In the case of elevated pressures ($p>1\,\text{atm}$), pressure broadening is given by

(27) $$\xi_{b,i} = \sum_{l=0}^{3}\sum_{m=0}^{M}\sum_{n=0}^{3} c_{lmn}\cdot\left(\frac{T_g\cdot T_b}{2500}\right)^n\cdot\xi_i^m\cdot\psi^{l+1},$$

whereas the elevated pressure influences the system through

(28) $$\psi = \ln\left(p_e\right),$$

with

(29) $$p_e = f(X_{H_2O}, X_{CO_2}, p),$$

which can be found in [13], p.23.

Note, that one uses either $\xi_{sb,i}$ or $\xi_{b,i}$ in Eq. (24). For CO_2 systems at atmospheric pressure, self-broadening is neglected, hence $\xi_{sb,i}(CO_2)=0$.

Figure 3 underlines the theory of the SLWSGGM, choosing reasonable intervals of C_{abs} first and obtaining the weight through $F(C_{abs,i})$ afterwards. In this work, the absorption cross sections are between $3\cdot10^{-5}\,\frac{m^2}{mol}$ and $60\,\frac{m^2}{mol}$ due to the validity of the correlation function.

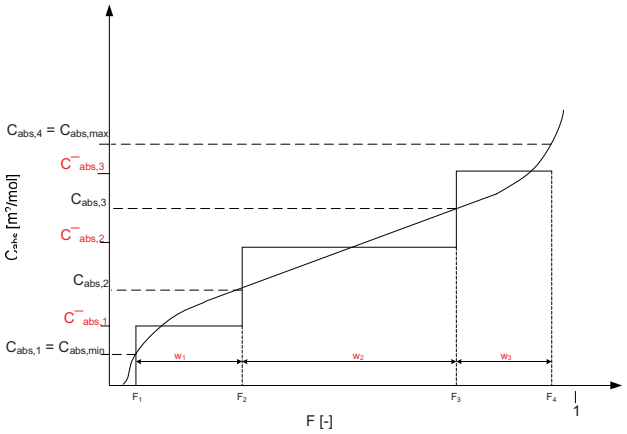

FIGURE 3. Mean absorption cross sections and weights for Denison/Webb's SLWSGGM for three gray gases

In the case of a mixture of H_2O and CO_2, the weight is obtained by multiplication of the singular weights [12], p. 789

(30) $$w_{i,k} = w_i\cdot w_k,$$

and the absorption coefficient is gained by a summation

(31) $$a_{i,k} = a_i + a_k.$$

Limitations of the SLWSSGM are summarized in Tab. 1.

3.5. Summary of Models

The WSGG models described above are summarized in Tab. 1.

Name	Species	Temperature Range [K]	Pressure Path-Length-/ Pressure-Range
Smith	H_2O H_2O/CO_2	600-2400	0.001-10 [Pa·m]
Copalle	H_2O/CO_2	2000-3000	0.01-3.5 [Pa·m]
Johans-son	H_2O/CO_2	500-2500	0.01-60 [Pa·m]
Denison /Webb	H_2O CO_2 H_2O/CO_2	500-2500	0.32-100 [10^5 Pa]

TABLE 1. Summary of WSGG Models

4. ANALYTICAL TOOL FOR TOTAL EMISSIVITY OF WSGG MODELS

To compare the WSGG models, the total emissivity is judged to be a suitable property. The total emissivity of a gas using the WSGGM is defined as

$$\varepsilon_g = \sum_{i=0}^{I} w_i(T) \cdot \left[1 - e^{(-a_i \cdot S)}\right]. \quad (32)$$

This expression is computed by an EXCEL tool with the input of static temperature T, static pressure p, molar fraction X of emitting species (H_2O and/or CO_2) and a path length S. For Denison's model the blackbody temperature T_b is assumed to be equal to the gas temperature T_g.

Figure 4 shows a plot of total gas emissivity over temperature for H_2O.

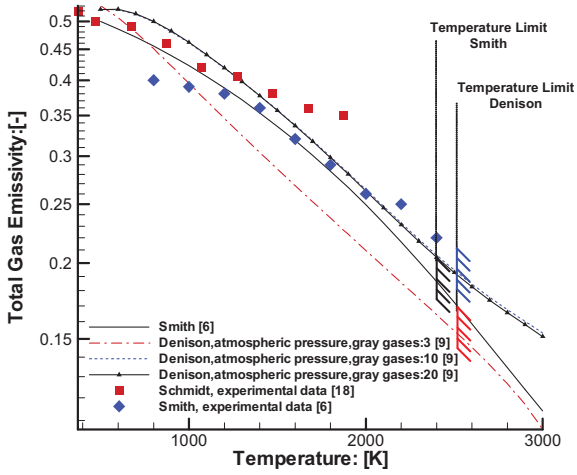

FIGURE 4. Total gas emissivity $\varepsilon_g \ (S = 1\,\mathrm{m})$ for H_2O $\left(X_{H_2O} = 1.0\right)$ at atmospheric pressure $\left(p = 1.01325 \cdot 10^5\,\mathrm{Pa}\right)$

It reveals that in H_2O systems at atmospheric pressure, the WSGGM of Smith approximates its experimental data best up to 2000 K. Denison's model is most accurate when ten or twenty gray gases are used and approximates Schmidt's experimental data best below 1400 K. It provides a better approximation than Smith's WSGGM for Smith's data above 1800 K. It is indicated by Fig. 4 that all models tend to unphysical behaviour when their validated maximum temperature is exceeded.

For a H_2O system at an elevated pressure of $101.325 \cdot 10^5\,\mathrm{Pa}$, Fig. 5 shows the total gas emissivity for $S = 1\,\mathrm{m}$.

There is a significant difference between the emissivity of Smith's WSGGM and Denison's SLWSGGM. As Smith's WSGGM is valid only at atmospheric pressure the results of Denison's model are assumed to be the most reasonable because it is validated up to $101.325 \cdot 10^5\,\mathrm{Pa}$. Nevertheless, a lack of experimental data at this pressure complicates this judgement. Again, an excess of temperature limits leads to an unexpected slope of total emissivity which has no physical reason.

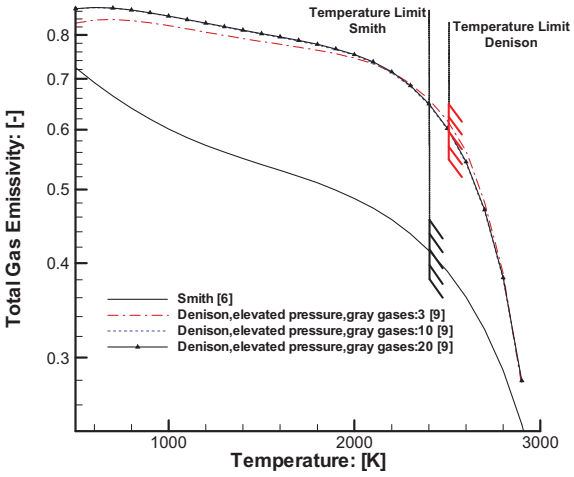

FIGURE 5. Total gas emissivity $\varepsilon_g \ (S = 1\,\mathrm{m})$ for H_2O $\left(X_{H_2O} = 1.0\right)$ at elevated pressure $\left(p = 101.325 \cdot 10^5\,\mathrm{Pa}\right)$

A mixture of H_2O and CO_2 is examined in Fig. 6 for atmospheric pressure and $S = 1.5\,\mathrm{m}$ as well as in Fig. 7 for elevated pressure and $S = 0.39\,\mathrm{m}$.

At atmospheric pressure, the WSGG models by Smith and Copalle approximate the data by Smith best up to their maximum validation temperature. Denison's and Johansson's models underestimate the total emissivity, whereas again Denison's SLWSGGM with ten gray gases supplies better results than the one with three gray gases.

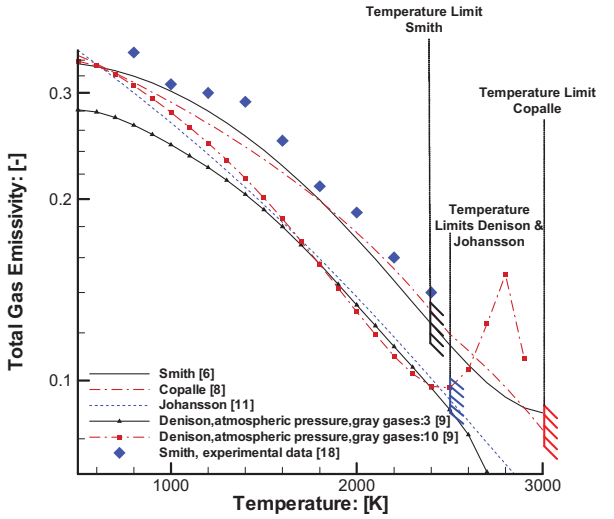

FIGURE 6. Total gas emissivity ε_g $(S = 1.5\ \mathrm{m})$ for H_2O/CO_2 mixture $\left(X_{H_2O} = X_{CO_2} = 0.1\right)$ at atmospheric pressure $\left(p = 1.01325 \cdot 10^5\ \mathrm{Pa}\right)$

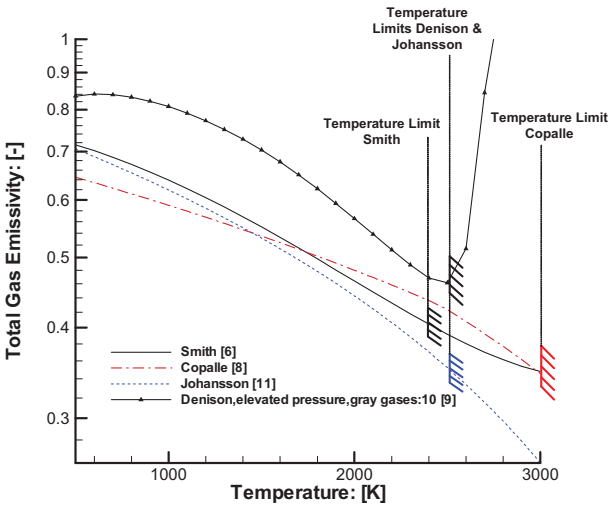

FIGURE 7. Total gas emissivity ε_g $(S = 0.39\ \mathrm{m})$ for H_2O/CO_2 mixture $(X_{H_2O} = X_{CO_2} = 0.1)$ at elevated pressure $\left(p = 101.325 \cdot 10^5\ \mathrm{Pa}\right)$

In the case of elevated pressure, the WSGG models again yield total emissivities below the estimate of Denison's SLWSGGM. As in the H_2O case, a judgement which estimate is most appropriate is difficult because experimental data is not existent. With regard to Denison's maximum pressure of $101.325 \cdot 10^5\ \mathrm{Pa}$, this model is again expected to be most suitable.

For the mixture of both species, the sensitivity towards temperature excess increases. For Denison's model this behaviour is caused by unphysical mixture weights $w_{i,k}$ which are sensitive to temperature excesses due to a multiplication of singular weights as Eq. (30) underlines. Also, Smith's model shows an unphysical increase in total emissivity above 2400 K.

It should be noted that the total emissivity plots depend on the path length, which determines the length of interaction between a photon and the surrounding gas. This path length is different for various geometries; hence the results herein are only valid at the given path lengths. The investigation of total emissivity at other path lengths is given in [13].

5. IMPLEMENTATION OF WSGG MODELS IN NSMB

The WSGGM and SLWSGGM described above are implemented in the CFD code NSMB. The order of calls for calculation of the spectral properties is given in Fig. 8. Depending on the value of the parameter *iradspmodel* the WSGGM/SLWSGGM is used as spectral model and the value of *iwsggmtype* decides which model is used. The final user input is to determine which species are considered in the model, e.g. by setting the variable *iwsggmsmith* for Smith's WSGGM.

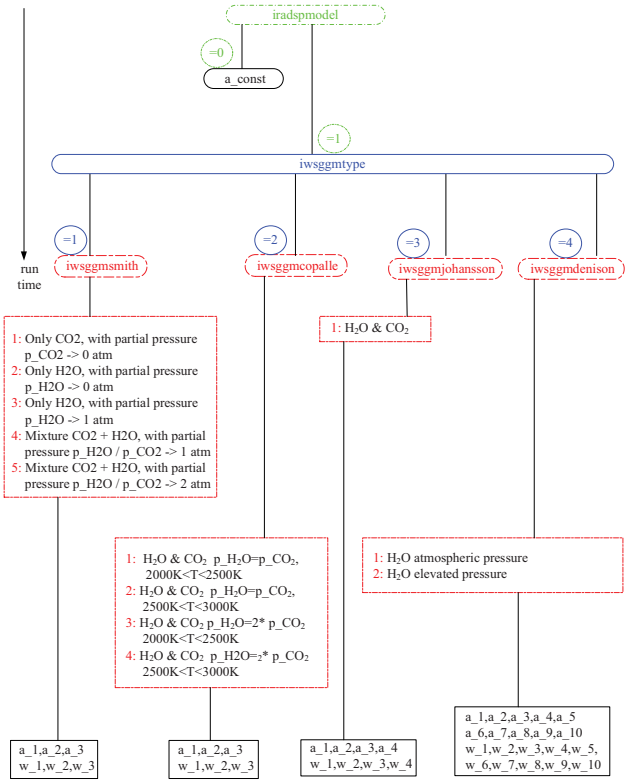

FIGURE 8. User inputs for spectral model and calculation of weights and absorption coefficients

6. CFD SIMULATION OF THE SSME MAIN COMBUSTION CHAMBER

With the implemented WSGG models, a CFD simulation is realised using the CFD code NSMB [15] as well as the commercial code CFX [16], in which the models have also been implemented [14].

The grid that is used for all studies is shown in Fig. 9. It consists of 16 blocks to accelerate convergence because each block is solved by one processor. The mesh distribution in radial direction, determining the spatial distribution of cells is exponential, meaning that the mesh gets finer (e.g. the distance between each cell is smaller) to enhance the resolution of wall boundary layers.

As each WSGG model is not usable for all combustion cases, validation of the models is used for two different cases. The first one is the classical H_2/O_2 combustion in the SSME MCC and the second is a CH_4/O_2 combustion. In the first case, H_2O is produced as contributor to radiative transfer. In the second one, H_2O as well as CO_2 influence the radiative transfer.

The first case with H_2/O_2 is done using NSMB and CFX, whereas NSMB uses Smith's WSGGM and CFX uses Smith's WSGGM and Denison's SLWSGGM. The second combustion case is done with Copalle's WSGGM and Denison's SLWSGGM in CFX. The results for CFX have been taken from [14].

All WSGG models used in the simulation are limited in temperature and some are also limited in pressure. Limitation in temperature is regarded to be essential preventing unphysical results as the total emissivity investigations show. Those models valid only at atmospheric pressure (Smith, Copalle) are used with and without limitation of pressure to investigate their off-design use.

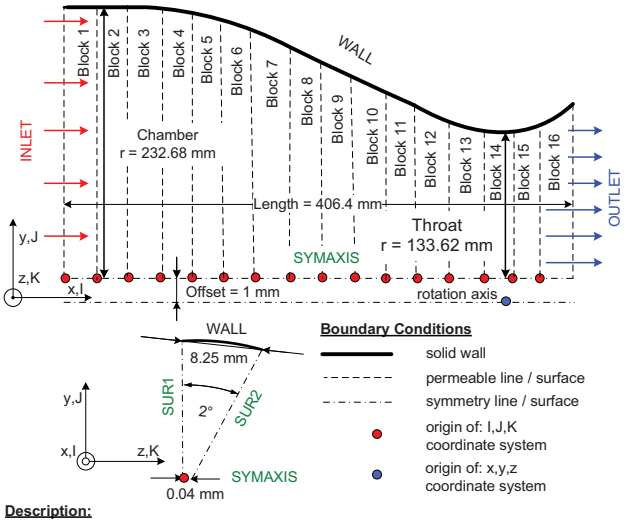

Description:

Mesh Type:
-> Hexahedral, total number of **cells**: 142848 (with K = 1) and 285696 (with K = 2)
-> CFX : Mesh is exported as unstructured mesh with K = 1 cell.
-> NSMB: Mesh is exported as Multiblock mesh (16 Blocks) with K = 2 cells.

Blocks 1-16:
-> Number of finite volume **cells**: I = 24; J = 372; K = 1 (CFX) or K = 2 (NSMB)
-> Nodes distribution in direction:

I:	J:	K:
Mesh law: uniform/exponential max. cell space = 1.7 mm	Mesh law: exponential cell space (j=1) = 0.50 mm cell space (j=372) = 1.5E-5 mm Max. growth ratio: 1.25	Mesh law: uniform cell space = variable

FIGURE 9: Mesh for the CFD simulation

The radiative transport models used in the simulation are the Rosseland Radiation Model (RRM) in NSMB and the Discrete Transfer Model (DTM) in CFX. The theory of both models especially combined with the WSGGM approach is complicated and will not be discussed herein. The RRM is explained in [17], p. 41 and details of the DTM are given in [1], p. 498.

6.1. H_2/O_2 Simulation

The models, boundary conditions and numerical parameters for the H_2/O_2 combustion for NSMB are given in [13, 17] and for CFX in [14].

To estimate the radiative wall heat flux (RWHF), the total emissivity of the gas in the SSME is illustrated in Fig. 10. As the total emissivity indicates which fraction of the maximum blackbody energy is actually emitted by a gas, a higher total emissivity causes higher radiative wall heat fluxes.

Based on the results in Fig. 10 it is assumed, that the RWHF for both Smith's and Denison's model at atmospheric pressure is nearly the same whereas Denison's model at elevated pressure will estimate the highest RWHF.

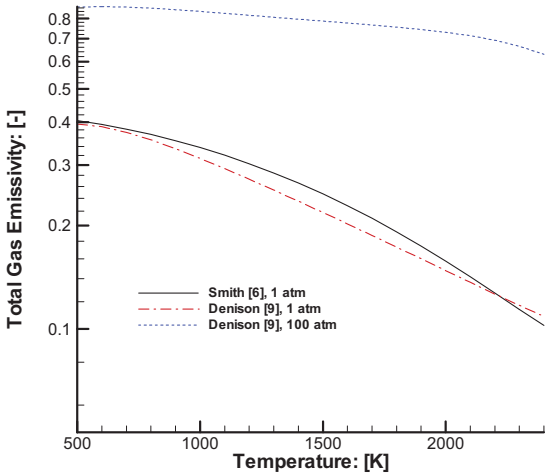

FIGURE 10. Total gas emissivity for the SSME MCC case using H_2/O_2 combustion

Figure 11 shows the RWHF over the axial distance. It reveals first of all that the RWHF using NSMB is almost one magnitude above the results of CFX. A reason for this is the different radiation transport model which shall be discussed in the last chapter.

The differences in the RWHF due to the WSGG models are investigated using the CFX simulations.

If the atmospheric models are used whose pressure is limited to $1.01325 \cdot 10^5 \mathrm{Pa}$ for calculation of the absorption coefficient in Eqs. (14) and (20), only small differences between Denison's model and Smith's model occur. The latter computes a smaller RWHF than Denison's model. Compared to benchmark simulations by Naraghi [3] and Wang [4], both models under-predict the RWHF.

Better results in terms of comparability to benchmark results are gained when employing models for elevated pressure. If Smith's WSGGM is used without pressure limitation, its RWHF approximates Wang's results best. Denison's SLWSGGM at elevated pressure gives the highest RWHF predictions and approximates Naraghi's results downstream from the throat best. After the throat, Smith's and Denison's model yield nearly the same results, both over-predicting the RWHF of the benchmarks.

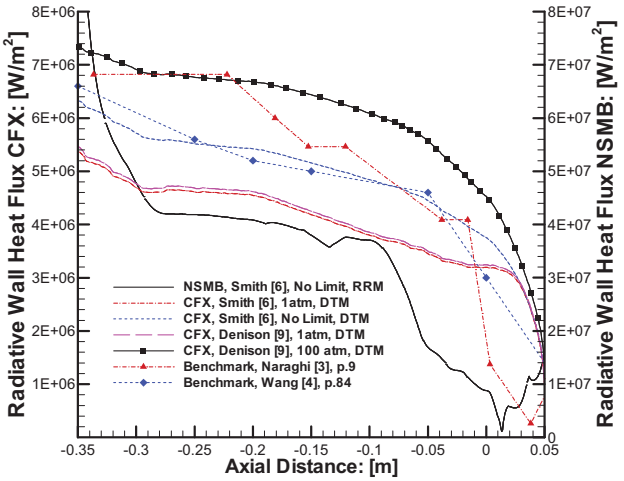

FIGURE 11. Radiative Wall Heat Flux for H_2/O_2 combustion and different WSGG models using NSMB and CFX

The results confirm the predictions based on the total emissivity plots. Denison's model at elevated pressure estimates the highest RWHF since its total emissivity is highest, too. At atmospheric pressure, Denison predicts nearly the same RWHF as Smith, according to a total emissivity which is almost identical.

6.2. CH_4/O_2 Simulation

For the CH_4/O_2 simulation no benchmarks are available. Therefore only the results of the CFD simulation with CFX are presented in Fig. 13. Although Smith and Johansson are capable to simulate the spectral properties for H_2O/CO_2 mixtures, only Copalle and Denison are chosen to be compared, because the total emissivity investigation revealed only small differences between Smith, Copalle and Johansson for CH_4/O_2 combustion.

To estimate the RWHF, the total emissivity of the combustion gases for this case is shown in Fig. 12. The horizontal line for Copalle's total emissivity results from its limitation in temperature between 2000 K and 3000 K. Therefore the total emissivity below 2000 K is limited to the value at 2000 K.

The results of Fig. 12 force the assumption that the radiative wall heat fluxes of both models at atmospheric pressure are close to each other and that the RWHF with Denison's SLWSGGM at elevated pressure is the highest.

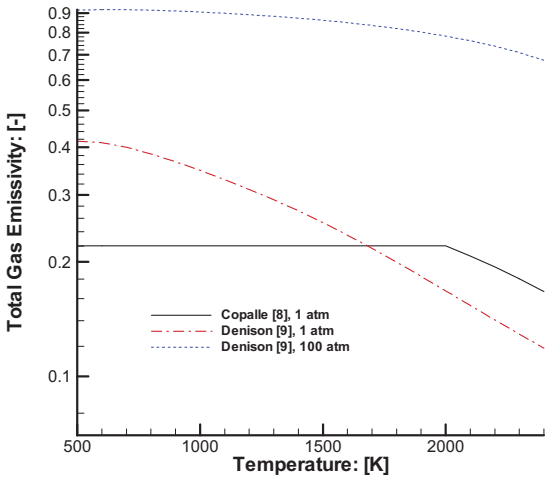

FIGURE 12: Total gas emissivity for the SSME MCC case using CH_4/O_2 combustion

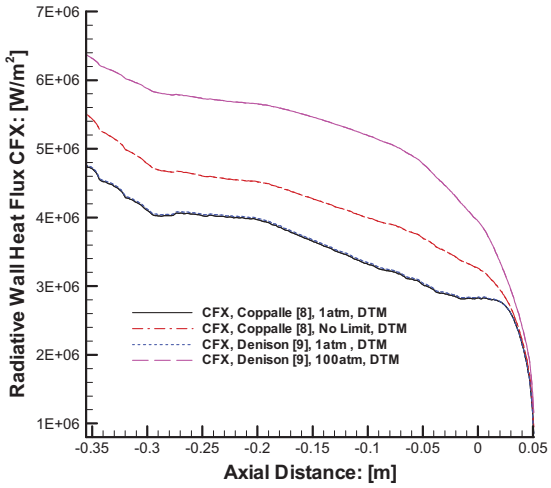

FIGURE 13: Radiative Wall Heat Flux for CH_4/O_2 combustion and different WSGG models using CFX

Again, the models at atmospheric pressure estimate the minimal RWHF. The differences between Denison and Copalle are small and Denison estimates the higher RWHF. At elevated pressure the difference increases and is about $10^6 \frac{\mathrm{W}}{\mathrm{m}^2}$ from the inlet up to the throat. Upstream from the throat the difference vanishes.

The predictions from the total emissivity investigations are confirmed in the CH_4/O_2 case too because Denison's model at elevated pressure yields the highest RWHF.

7. SUMMARY OF RESULTS

The aim of this study is to identify suitable WSGG models for application in combustion systems like rocket motors. These models approximate the absorption coefficient for several spectral regions and thus minimize computational efforts compared to line by line calculations. For H_2/O_2 combustion, the models by Smith and Denison and for CH_4/O_2 combustion those by Smith, Copalle, Johansson and Denison are investigated.

Concerning their theoretical basis, the models by Smith, Copalle and Johansson are the simplest while Denison's model as it is investigated herein using a correlation function is more complicated. Nevertheless, the model by Denison is validated up to elevated pressures of $101.325 \cdot 10^5$ Pa whilst the other models are limited to atmospheric pressure. The common disadvantage of all WSGG models is their limitation in temperature. The maximum temperature of the models is 2500 K for H_2/O_2 systems and 3000 K for CH_4/O_2 systems which is comparable low for typical rocket engine combustion scenarios.

To analyse and compare the quantitative and qualitative results of the WSGG models, the total emissivity over temperature is compared for different pressures, path lengths and species first.

For H_2/O_2 at atmospheric pressure, the study reveals that Denison's and Smith's models deliver results close to experimental data even though both cannot reproduce the data over the entire temperature range. Further it becomes obvious that Denison's model, which does not prescribe a certain number of gray gases, is most suitable when 10 gray gases are used. At elevated pressure the differences in total emissivity between Denison's and Smith's models increase. As Smith's model is validated only at atmospheric pressure, the results of Denison are considered more trustworthy because of its validity at pressures up to $101.325 \cdot 10^5$ Pa .

The results for CH_4/O_2 are similar to those of the H_2/O_2 system. At atmospheric pressure all models are close to each other while Smith's and Copalle's models approximate the experimental data best. Denison's model is again recommended to be used with at least 10 gray gases. At elevated pressure, this model is also expected to be the most reliable one.

What the total emissivity investigation clearly emphasizes is the limitation of all models in temperature. The total emissivity tends to unphysical values if the permitted maximum temperature is exceeded. As a result, all WSGG models are limited to their reliable temperature range when implemented in the CFD codes NSMB and CFX.

As a second analysis, the WSGG models are examined in a CFD simulation of the SSME MCC using the CFD codes NSMB and CFX.

Comparing the results of NSMB (radiation transport model: RRM) and CFX (radiation transport model: DTM) for H_2/O_2 combustion using Smith's WSGGM reveals that the RWHF is different almost by one magnitude. One reason for this is the radiation transport model in conjunction with the WSGGM. In the RRM the effective radiative heat flux depends on the sum over the fraction $\frac{w_i}{a_i}$, known as the Rosseland mean absorption coefficient, whereas in the DTM the radiative heat flux depends on the Planck mean absorption coefficient which is the sum over $w_i \cdot a_i$. The analytical EXCEL tool emphasizes these dependencies, as the Rosseland mean absorption coefficient is almost half a magnitude above the Planck mean absorption coefficient. Thus its radiative wall heat flux is expected to be higher.

With one specific radiation transport model (DTM) used in CFX, all WSGG models predict a different RWHF in both the H_2/O_2 and CH_4/O_2 combustion. For the H_2/O_2 case the models by Smith and Denison approximate the benchmark data sufficiently. Smith's model can be used above its maximum pressure without a loss of accuracy and Denison's model for elevated pressure should also be used for this combustion system. The CH_4/O_2 case with Copalle's and Denison's models shows that the RWHF in general is smaller than in the H_2/O_2 system. This is due to a smaller temperature of the combustion gases in the CH_4/O_2 case that is caused by a smaller specific energy of CH_4 (50 MJ/kg) compared to H_2 (143 MJ/kg). Due to a lack of benchmark data it cannot be judged which model is appropriate for CH_4/O_2 combustion. Nevertheless, using Copalle's model above atmospheric pressure does not lead to unphysical results although the RWHF is smaller than the one predicted by Denison.

In the focus of computational costs the WSGG models by Smith, Copalle and Johansson need less CPU time than the SLWSGGM by Denison because of its extensive correlation functions. Compared to a simulation without radiation in CFX, the use of the DTM combined with Smith's WSGGM increases the CPU time by 400 %. In contrast, Denison's SLWSGGM increases the CPU time by 990 % [17]. Besides, the CFD simulation underlines that the results of the models by Smith and Copalle are comparable to the benchmark and Denison's model respectively. Thus it is recommended to use those models or Johansson's model to gain accurate results with least computational efforts.

8. FURTHER STUDY

To enhance the capabilities of NSMB in radiative transfer simulations, the P1 model has to be implemented which is known to provide better results than the RRM. For the spectral modelling, other models than the WSGGM/SLWSGGM can be used, e.g. the FSK by Modest [1], p. 616. If Denison's model is used, a direct link to the line by line spectra is assumed to be faster than the correlation approach used in this study.

REFERENCES

[1] M. F. Modest, Radiative Heat Transfer, Second Edition ed., Academic Press, San Diego (USA), London (UK), Burlington (USA), 2003.

[2] H. C. Hottel and A. F. Sarofim, Radiative Transfer, McGraw-Hill Book Company 1967.

[3] M.H. Naraghi, S. Dunn and D. Coats, Modeling of Radiation Heat Transfer in Liquid Rocket Engines, AIAA-2005-3935, 2005

[4] T.-S. Wang, Multidimensional Unstructured-Grid Liquid Rocket-Engine Nozzle Performance and Heat Transfer Analysis, Journal of Propulsion and Power, Vol. 22, No. 1, pp. 78-84, 2006.

[5] D. Birgel and F. Göbel, CFD Simulation of Hydrogen-Oxygen System for Space Shuttle Main Combustion Chamber including Radiative Effects, Institute of Thermodynamics, Universität der Bundeswehr München, 2009.

[6] T. F. Smith, Z. F. Shen, and J. N. Friedman, Evaluation of Coefficients for the Weighted Sum of Gray Gases Model, ASME Journal of Heat Transfer, Vol. 104, pp. 602-608, 1982.

[7] F. Göbel, D. Birgel, A. Thellmann, CFD Simulation of Hydrogen-Oxygen and Methane-Oxygen System for Space Shuttle Main Combustion Chamber including Radiative Effects, 60th International Astronautical Congress of the International Astronautical Federation, IAC-09-E2.2.9, Daejeon (Korea), 2009

[8] A. Coppalle, The Total Emissivities of High Temperature Flames, Combustion and Flame, Vol.49, pp. 101-108, 1983.

[9] M. K. Denison and B. W. Webb, An Absorption-Line Blackbody Distribution Function for Efficient Calculation of Total Gas Radiative Transfer, Journal of Quantitative Spectroscopy & Radiative Transfer, Vol. 50, pp.499-510, 1993.

[10] R. Siegel and J.R. Howell, Thermal Radiation Heat Transfer - 4th ed., Taylor & Francis 2002.

[11] R. Johansson, Account for Ratios of H_2O to CO_2 in the Calculation of Thermal Radiation of Gases with the Weighted-Sum-of-Grey-Gases Model, Proceedings of the Sixth Mediterranean Combustion Symposium, 2009.

[12] M.K. Denison and B.W. Webb, The Spectral-Line Weighted-Sum-of-Gray-Gases Model for H_2O/CO_2 Mixtures, Journal of Heat Transfer, Vol. 117, No. 3, pp. 788-792, 1995

[13] F. Göbel, Implementation of Spectral Models for Gas Radiation into the CFD Solver NSMB and Validation on the basis of the SSME Main Combustion Chamber, Diploma Thesis, Institute of Thermodynamics, Universität der Bundeswehr München, 2009.

[14] D. Birgel, CFD Simulation of the SSME Main Combustion Chamber operated by H2-O2 and CH4-O2 with CFX and FLUENT including Thermal Gas Radiation, Diploma Thesis, Institute of Thermodynamics, Universität der Bundeswehr München, 2009.

[15] J.B. Vos et al., NSMB Handbook 4.5, CFS Engineering, Lausanne, 2007.

[16] ANSYS CFX 11.0, ANSYS CFX Introduction, 2006.

[17] A. Thellmann, Impact of Gas Radiation on Fluid Dynamics, in particular on Wall Heat Loads, in Hydrogen-Oxygen vs. Methane-Oxygen Systems, based on the SSME Main Combustion Chamber, PhD Thesis in preparation, Institute of Thermodynamics, Universität der Bundeswehr München, 2010.

[18] E. Schmidt, Messung der Gesamtstrahlung des Wasserdampfes bei Temperaturen bis 1000℃, Zeitschrift Technische Mechanik und Thermodynamik 3, pp. 57-70, 1932.